Chapter 14

Modeling of Novel Plasma-Optical Systems

Iryna Litovko and Alexey Goncharov

Additional information is available at the end of the chapter

http://dx.doi.org/10.5772/intechopen.77512

Abstract

This is the review of the current status an ongoing theoretical, simulations and some experimental researches of the novel plasma dynamical devices based on the axial-symmetric cylindrical electrostatic plasma lens (PL) configuration and the fundamental plasma-optical principles of magnetic electron isolation and equipotentialization magnetic field lines. The crossed electric and magnetic fields plasma lens configuration provides us with the attractive and suitable method for establishing stable plasma discharge at low-pressure. Using plasma lens configuration in this way some novel cost-effective, low-maintenance, high-reliability plasma devices using permanent magnets were developed. In part, it was proposed and created device for ion treatment and deposition of exotic coatings, device for filtering dense plasma flow from micro-droplets, electrostatic plasma lens for focusing and manipulating wide aperture, high-current, low-energy, heavy metal ion plasma flow, and the effective lens was first proposed for manipulating high-current beams of negatively charged particles (negative ions and electrons). Here we mainly describe models and results of theoretical consideration and simulation of the novel generation cylindrical plasma devices.

Keywords: plasma lens, plasma accelerator, space charge, ion beam, electron beam, beam transport

1. Introduction

The electrostatic plasma lens (PL) is a well-investigated tool for focusing and manipulating large area, high-current, moderate energy ion beams, where the concern of beam space charged compensation is critical. The fundamental concept of the PL was first described by Morozov [1]. It is based on application of the plasma-optical principles of magnetic insulation of electrons and equipotentialization of magnetic field lines for the control of electric fields introduced into the plasma medium [2].

These kinds of devices are part of a larger sort of plasma devices (plasma accelerators, ion magnetrons, thrusters, plasma lenses, etc.) that use a discharge in crossed electric and magnetic fields with closed electron drift for the generation, formation, and manipulation of intense ion beams and ion plasma flows. In accordance with the basic idea of plasma optics [1], spatial over thermal E-fields can be introduced in the plasma medium of an intense ion beam, which makes possible high-current ion beams manipulation and focusing including beams of heavy ions. An idea to use the space charge for that purpose appeared to be very fruitful and successful [2, 3]. A number of effective plasma lenses for positive ion beams focusing were made and tested. The robust construction, low-energy consumption, and high-cost-effectiveness make these tools attractive for practical applications.

Some new ideas for using these plasma-optical principles for creation axial symmetric high-current mass separation devices were described firstly in [4]. Note also that this approach is appropriate for the creation of linear or curved magneto-electrostatic plasma guiding ducts for use in vacuum-arc plasma filtering system. Following these plasma-optical principles, changing the magnetic field line configuration and the distribution of electric potential enables the formation and control of high-current ion beams while maintaining their quasi-neutrality. This makes the application of such devices attractive for the manipulation of high-current beams of heavy ions.

The plasma lens configuration of crossed electric and magnetic fields provides a suitable and attractive method for establishing a stable discharge at the low-pressure. Using plasma lens configuration in this way were elaborated, explored and developed some cost efficiency, low-maintenance plasma devices for ion treatment, and deposition of exotic coatings with given functional properties. These devices make using of permanent magnets and possess considerable flexibility with respect to spatial configuration. They can be operated as a stand-alone tool for ion treatment of substrates, or as part of integrated processing system together with cylindrical magnetron sputtering system, for coating deposition. The cylindrical plasma-optical magnetron sputtering device with virtual anodes and cylindrical plasma production device for the ion treatment of substrates with complicated cylindrical was proposed and created [5–7]. These devices can be applied both for fine ion cleaning and activation of substrates before deposition and for sputtering.

One particularly attractive result of this background work was observation of the essential positive potential at the floating substrate treated by cylindrical ion cleaning device. This suggested to us the possibility of an electrostatic plasma lens for focusing and manipulating high-current beams of negatively charged particles (electrons and negative ions) that is based on the use of the cloud of positive space charge in conditions of magnetic insulation electrons. The idea of the plasma lens based on electrostatic electron isolation for creation positive space charge was first proposed in [8]. Later, it was proposed to use magnetic electron insulation for creation of a stable positive space charge cloud [9].

Here we describe computer modeling for some of these novel plasma-optical systems.

http://dx.doi.org/10.5772/intechopen.77512

2. Plasma lens with a positive space charge cloud for focusing intense negative charged particle beams

2.1. Model description

The plasma lens is a cylindrical plasma accelerator with an anode layer and used as a device with magnetic insulation of electrons for creation of the dynamic cloud of positive space charge. The scheme of the plasma lens with magnetic insulation used for creation of the dynamic cloud of positive space charge is shown in **Figure 1a**.

The lens has a system of permanent magnets that produce an axially symmetric magnetic field between the poles of a magnetic circuit serving as cathode. The magnetic field is controlled by varying the number of magnets. The magnetic field configuration is typical for the single magnetic lens configuration, because of the lens could focus the transported electron beams. When a positive potential is applied to the anode, a discharge in the axial magnetic, and radial electric crossed fields is ignited between the anode and the cathode. The electrons are magnetized in anode layer and drift along closed trajectories in the azimuthal direction, repeatedly ionize atoms of the working gas, and gradually diffuse to the anode. The ions thus formed are accelerated in the strong electric field created by the electron space charge and leave the ion source through a hole in the acceleration channel. The fast ions reach the system axis and accumulate in the region around it, as it schematically shown in **Figure 1b**. In this way, the axially converging ion beam creates a positive space charge. In the experiments, the energy of the argon ions converging beam could reach 2.5 kV. Maximum potential will be in the center on cylindrical axis. Ions are stored in the cylinder volume until their own space charge creates a critical electric field. This field forces ions to leave the volume, and the system comes to dynamic equilibrium after some relaxation time.

Electrons are magnetized in the anode layer, so their influence on ion dynamics can be neglected. The ion flow coming through the cylindrical surface will be equal to ions streaming down from the axis and leaving the cylindrical volume under action of the Coulomb force of their own space charge. Therefore, the set of equations describing this process in the cylindrical

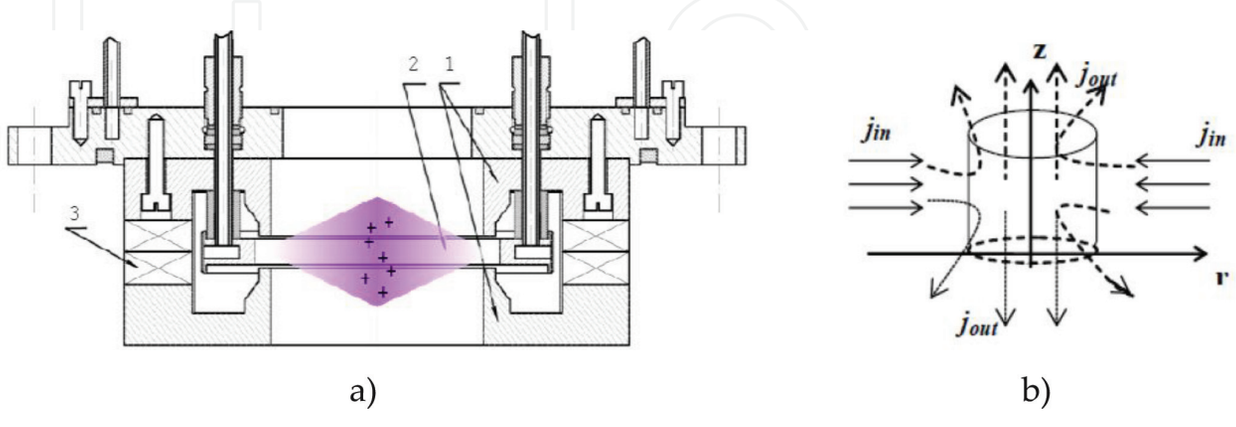

Figure 1. (a) Scheme of the plasma lens with magnetic electron insulation: 1 – cathode; 2 – anode; 3 – magnetic system based on permanent magnets; (b) Scheme the positive space charge cloud creation.

coordinate system can be written in the form that includes the Poisson, particles motion, and continuity law equations:

$$\frac{1}{r}\frac{\partial}{\partial r}\left(r\frac{\partial U}{\partial r}\right)+\frac{\partial^2 U}{\partial z^2}=-4\pi q_i n_i \tag{1}$$

$$M_i\frac{dv_i}{dt}=q_i E+\frac{1}{c}[v_i\times B] \tag{2}$$

$$V_i\cdot\left(\frac{\partial n_i}{\partial t}+div\left(j_{out}\right)\right)=S\cdot j_{in} \tag{3}$$

where M_i, q_i, v_i, n_i are ion mass, charge, velocity, and ion density, respectively, E – electric field: $E_r=-\partial U/\partial r$, $E_z=-\partial U/\partial z$, U – potential, B – magnetic field, V – cylindrical volume, j_{in} – current density at the boundary of current-collecting surface S of radius r and height h, and j_{out}– the ion current density leaving the cylindrical volume V. Knowing the space charge distribution, we can determine the expulsive force that acts on the particle on the boundary of space charge volume and calculate ions trajectories.

We can obtain estimations for electrical field and space charge in cloud in stationary case with simplifying assumptions. Let us suppose uniform ion distribution and that they enter to the cylinder perpendicular to its lateral surface and leave it along z-axis under action of electric field created by the ions own space charge. Thus considering of one-dimensional ions motion along the radius, we can write equation for potential in form:

$$\varphi_r''=\frac{4\pi j_{in}}{\sqrt{2q_i(\varphi_0-\varphi(r))/M_i}} \tag{4}$$

Solving it, we get solution similar to the low 3/2:

$$\left(\varphi_0-\varphi(r)\right)^{3/2}\approx\frac{9\pi j_{in}}{\sqrt{2q_i/M_i}}r^2$$

and obtain estimation for electric field:

$$E_r=-\frac{\partial\varphi}{\partial r}\approx\frac{4}{3}\left(\frac{9\pi j_{in}}{\sqrt{2q_i/M_i}}\right)^{2/3}r^{1/3}.$$

Let us now consider a cylindrical layer of ion space charge with radius r and assume that the ions leave it along z-axis, then neglecting radial coordinate we can write Poisson equation in layer in form: $\varphi_z''=4\pi\rho$, where $j_{out}=\rho\upsilon$. In stationary case from (Eq.(3)), we obtain: $j_{in}=r\frac{\partial j_{out}}{2\partial z}$. Integrating this expression with using expression $\upsilon=\sqrt{2q_i(\varphi(z)-\varphi(z'))/M_i}$ for velocity of ions leaving the layer, we obtain expression for the distribution of ion space charge density in form: $\rho\approx\frac{2j_{in}}{r\sqrt{2q_i(\varphi(z)-\varphi(z'))/M_i}}z$. Substituting last expression in Poisson equation for the layer and

solving it we get that potential and space charge density in layer is proportional to next expressions:

$$\varphi(r,z) \approx \left(j_{in}/r\right)^{2/3} z^2, \rho \approx 2\left(4\pi \frac{j_{in}}{r\sqrt{2q_i/M_i}}\right)^{2/3} \tag{5}$$

Substitute character system parameters we obtain estimations for ion density: n$\sim 10^{10}$ cm$^{-3,}$ and for electric field strength about 1000 V/cm, that is sufficient for high-current electron beam focusing.

Eqs. (1)-(3) were solved numerically by particle in cell (PIC)-method [10]. Every time interval Δt (that corresponded to the actual time interval approximately equal to $4{\cdot}10^{-8}$ sec) N new particles of charge q_i and mass M_i come to the volume considered. The magnitudes of N, Δt, q_i satisfy the relation: $\frac{Nq_i}{\Delta t} = j_i S$. Let us suppose that particles with energies from 0 to ε_{max} are distributed according to law:

$$N(\varepsilon) \approx \frac{1}{\sqrt{2\pi}\langle\varepsilon\rangle} \exp\left(-\frac{(\varepsilon-\varepsilon_0)^2}{2\langle\varepsilon\rangle}\right) \tag{6}$$

where $\varepsilon_0 = \varepsilon_{max}/2$ and $< \varepsilon >$ is average energy. They moved from cylinder surface to the system axis with the angular distribution according to cosine law: N(Θ)/N(0) ≈ cos (Θ), where N(Θ) are quantities of ions going out under angle Θ, N(0) is angular distribution amplitude. It should be noted that the distributions above are inherent to this kind of plasma accelerators with anode layer. As the first step the potential was specified at the anode, and the Laplace equation was solved. After that, the particles were launched and the equations of motion (Eq. (2)) for particles in the magnetic and calculated electric field were solved. The time step for motion equation solving was $\Delta\tau \ll \Delta t$ (about 10^{-11} sec). After time Δtby collecting of all particles with the use the "cloud in cell" method [10], the densities distributions of ions were calculated. The Poisson equation has been solved and electric field potential U(r, z) was calculated for this time moment. Electric field was calculated by the distribution of total space charge. After that in corrected electric field, the calculation of particles motion was resumed, and introducing the new portion of ions was performed. Equations of motion were solved both for "new" particles and for those that still left in the volume. **Figure 2** shows calculated

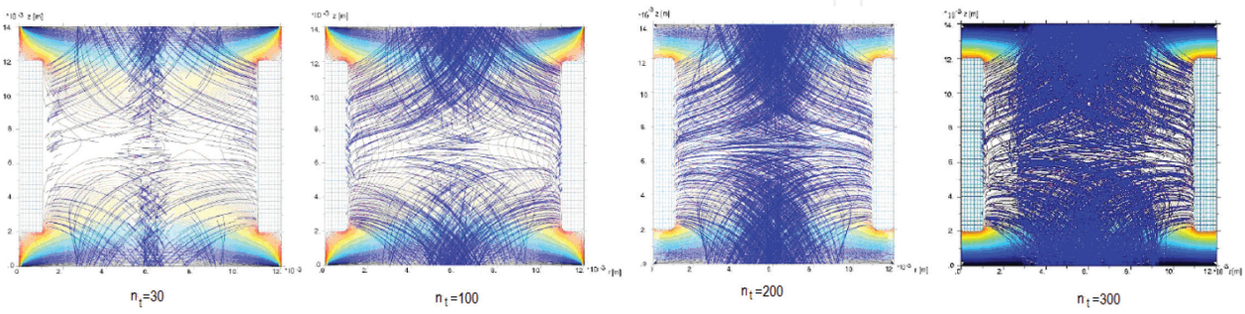

Figure 2. Positive space charge cloud formation and Ar+ ions trajectories for different time step.

Ar + ions trajectories in different time step. The calculation continued until reaching a self-consistent solution. The calculation time comprised 10^{-5} sec. For that time the stationary state of the lens operation was achieved.

2.2. Simulation results

The model was applied for calculating the lens volume based on the local area with diameter of 80 mm and a height of 50 mm. In our simulations, we considered Ar^+ and Xe^+ ion beams with maximal energy from 1 to 3 keV and total current of 20 mA that moved in the magnetic field. Magnetic field is similar to the experimental one and changes from 0.07 T near electrodes to 0.01 T on the system axis. The results of the calculations of the potential distribution when steady-state dynamical equilibrium is reached for Ar^+ ions with maximal energy 1.2–2.4 keV are shown in **Figure 3**. One can see that with ions energy increasing, the spatial distribution shape changes markedly. Whereas maximum of potential for ion beam's energy 0–1.5 keV (see left **Figure 3**) is double-humped situated in the coaxial region around the axis, the maximum for energy 0–2.4 keV (right) is single-humped onto the axis.

The same result we can see with ion mass increasing (see **Figure 4**). The maximum of potential for Ar + ion beam (**Figure 4** left) is in the coaxial region around the axis, but the maximum for

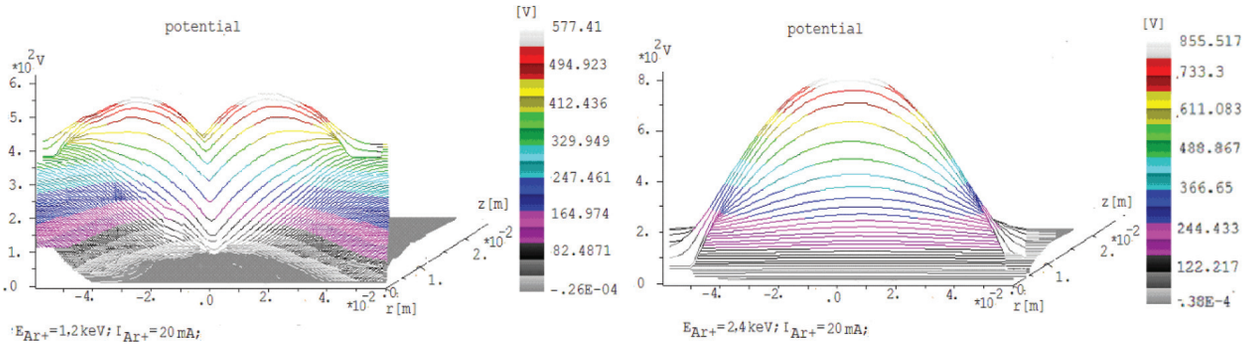

Figure 3. Potential distribution in plasma lens midplane for Ar + ion beam with total current 20 mA and E_{max} = 1.2 keV (left) and 2.4 keV(right).

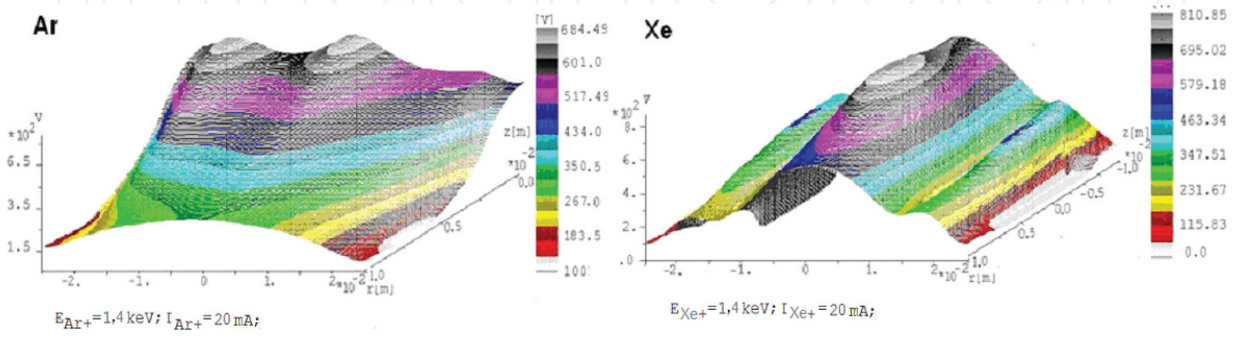

Figure 4. Potential distribution for Ar+ ion beam (left) and Xe+ ion beam (right) with total current 20 mA and E_{max} = 1.4 keV.

heavier Xe + ions (**Figure 4** right) is at the axis. This can be explained by a smaller influence of the momentum aberration on the converging Xe + ion beam dynamics.

The calculated ion density that could accumulate around system axis reaches 10^9–$2.7{\cdot}10^{10}$ $cm^{-3,}$ and electric field strength was up to 600 V/cm that is sufficiently for focusing intensive negative charged particle beams and correspond to our estimations. Thus the possibilities formation of the stable space charge cloud was demonstrated, and next task is to consider negative charge particle beam transport through space charge PL.

2.3. Negative charge particle beams focusing on space charge plasma lens

We investigated transport electron beam with energy from 5 to 20 keV through the plasma lens. As first step was solved equations for ion's part and as result – obtaining stable positive charge cloud inside plasma lens. Next step was launch e-beam through the lens with cloud. For correct description, we must solve equations for ions and electrons parts together, so we must include electron motion equations in our consideration and modify Poisson equation to form:

$$\frac{1}{r}\frac{d\varphi}{dr}+\frac{d^2\varphi}{dr^2}+\frac{d^2\varphi}{dz^2}=4\pi e(n_e+n_{eb}-n_i) \tag{7}$$

For simulation high-current electron beam transport need also taking into account the space charge of the particle and the magnetic self-field that may affect the dynamic beam particles in addition to the external fields. The possibility of ionization residual gas by electron beam is necessary taking into account also.

Equations of motion for electrons are solving by current tubes of variable width with central trajectory. A shape of trajectories in an electromagnetic field is calculated using Boris scheme [11]. A space charge beam density is calculated using equation of continuity: $div(\rho_e v_e) = 0$.A self-consistent solution can be found by repeated solving of Poisson equation, motion equations for all particles, and re-determination of the space charge distribution on every time step. An iteration method with relaxation was used for faster convergence.

Numerical simulations results show clearly that for electron beam current less than 1A the electrostatic beam focusing occurs [12, 13]. The results of simulation for space charge plasma lens and magnetic lens (ML) with the same magnetic field are shown in **Figure 5**. The comparison shows that beam compression is stronger, and beam divergence is less in PL case than in ML case. The experimental results [12, 13] confirm our simulations. The lens can be used even more effectively for negative ions beam focusing. The simulation results for H-beam with passing through plasma lens and magnetic lens with the same magnetic field are shown in **Figure 6**. One can see that lens effectively compresses H-ions beam, whereas the magnetic lens does not focus it at all.

However, it should be noted, some part of cloud ions can be captured by a beam and carried away from the cloud. It is positive for beam transport, but as a result of this, cloud potential decreases, and its focusing properties deteriorate. It is not critical for electron beams with current up to 1 A, because a new Ar + ions come to the cloud and renew its focusing properties.

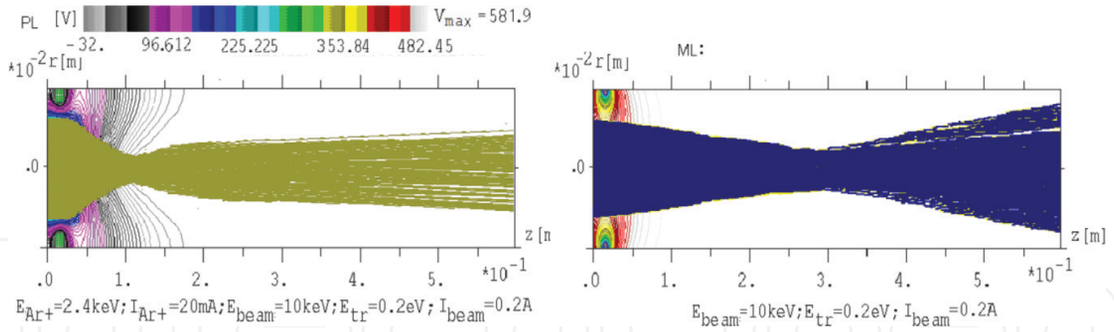

Figure 5. Electron beam (E_b = 10 keV, I_b = 0.2A) passing through the positive space charge plasma lens (left) and magnetic lens (right).

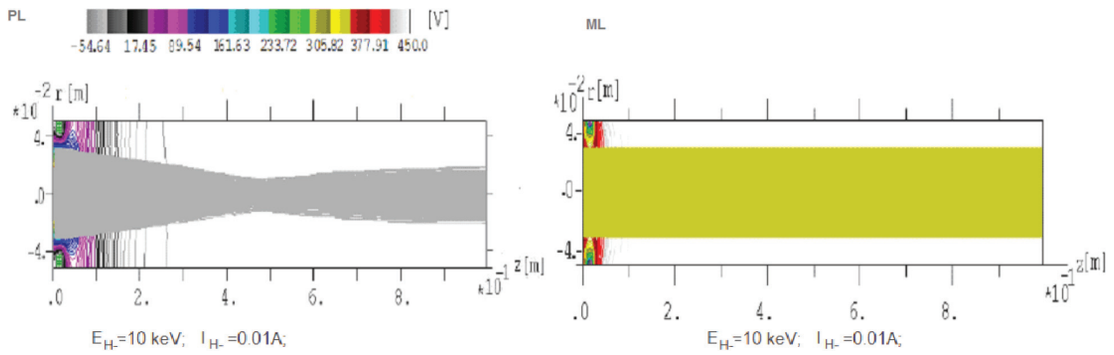

Figure 6. Trajectories of H-ions beam (E_b = 10 keV, I_b = 0.01A) passing through the positive space charge plasma lens (left) and magnetic lens (right).

However, for beam current of about or more 1 A the potential maximum in the positive space charge region decreases (from 580 to 210 V for I_{eb} = 1 A), the distribution is getting double-humped and electrostatic focusing destroyed (see **Figure 7** top).

It is due to that some part of ions comes out from cloud with the propagating electron beam and their number grows with beam current increasing [13]. A significant part of cloud particles carry out by e-beam along beam line, and ions are continuing to come in cloud from electrodes cannot support renewal processes. Thus cloud potential decrease and it distribution changes from one-hump to two-humps. Note that if it corresponded to case when beam space charge density a bit exceeds to space charge cloud density is possible to improve plasma lens electrostatic focusing property by increasing energy and current density Ar + ions beam that creates positive space charge cloud. **Figure 7** (down) shows potential distribution by electron beam propagating for increasing Ar + ions beam current from 20 up to 60 mA. One can see potential distribution come back to one-peak form and focusing properties of plasma lens recovered.

However, the positive space charge cloud quickly destroys with further increasing of electron beam current when beam space charge density significantly exceeds space charge cloud density, (see **Figure 8**) and it is not possible to renew electrostatic focusing properties anymore. In this case, for an electron beam with current on the order of tens of ampere for which the beam space charge density much more than space charge plasma lens the only the magnetic focusing

http://dx.doi.org/10.5772/intechopen.77512

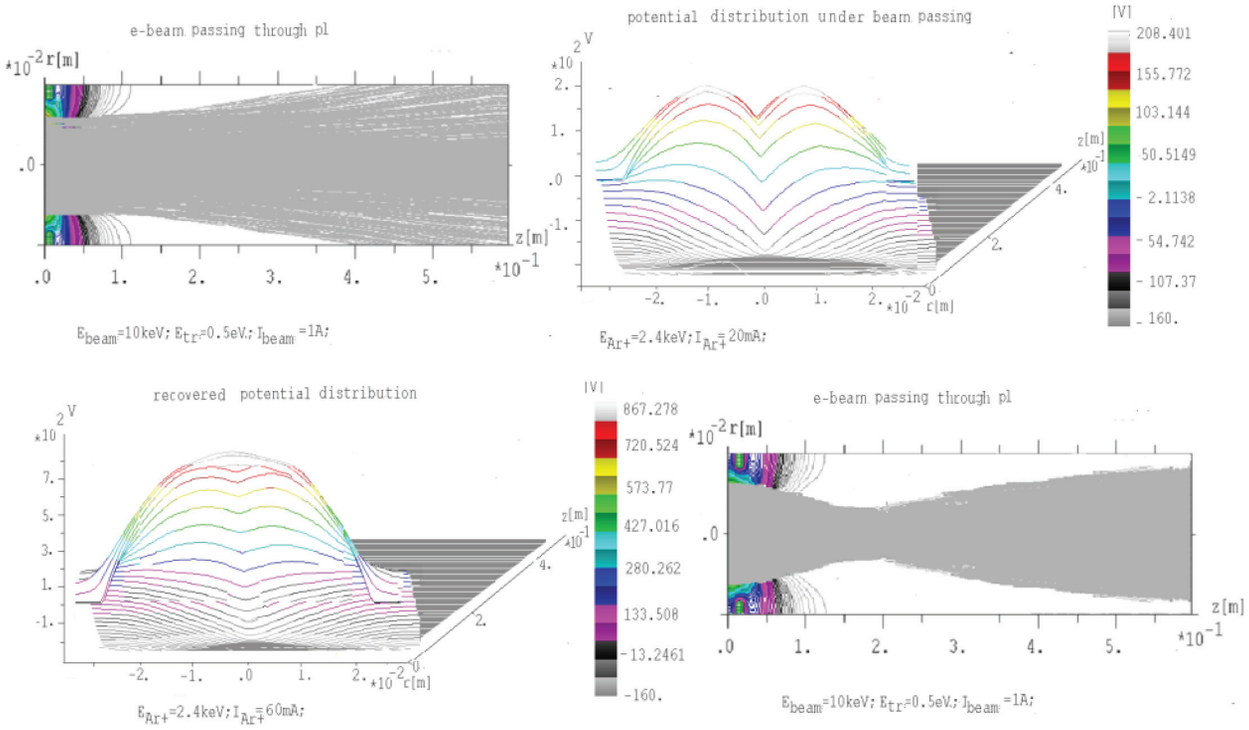

Figure 7. Electron beam trajectories (E_b = 10 keV, I_b = 1A) and positive charge cloud potential distribution created by Ar + ions beam with maximal energy 2.4 keV and current I = 20 mA(up) and I = 60 mA(down).

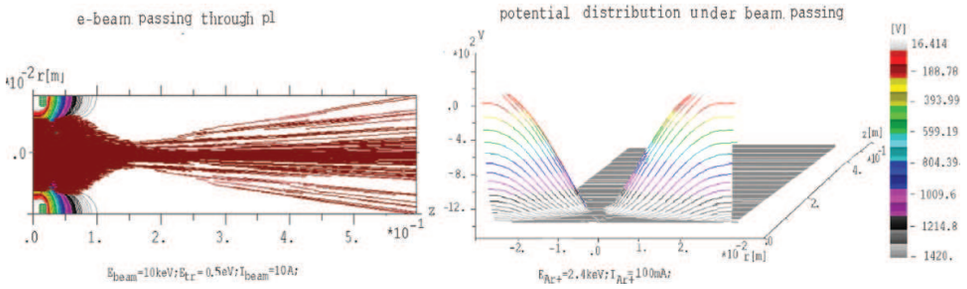

Figure 8. Electron beam trajectories (E_b = 10 keV, I_b = 10A) and positive charge cloud potential distribution created by Ar + ions beam with maximal energy 2.4 keV and current I = 100 mA. Magnetic field twice as much compared with previous case.

of the beam provides. However, even in this case use of PL is useful since it improves e-beam transport, providing additional compensation of beam space charge and decreasing beam divergence. Note that taking into consideration an ionization residual gas by electron beam do not lead to essential changing in simulations of final results.

2.4. Conclusion remarks

The research described has shown a principal possibility of creation of a positive space charge in the cylindrical anode layer accelerator due to a positive ion flow that converges onto its axis. This makes possible to develop a plasma lens with essentially under-compensated positive

space charge. The lens will be used for focusing and manipulating beams of negatively charged particles. The value of positive charge potential formed at the axis and the steady state of the space charge depending on plasma dynamical parameters of the system are determined experimentally [12, 13]. Electric field value reaching 600–1000 V/cm realized under experimental condition is determined. Such electric field strength is sufficient for creation of short-focus elements to be used in systems for manipulating intense beams of negative ions and electrons. Experimental results [14] demonstrate an attractive possibilities application positive space charged plasma lens with magnetic electron insulation for focusing and manipulating wide-aperture high-current no relativistic electron beams. For relatively low-current mode for which electron beam space charged less than positive space charged plasma lens, it realizes electrostatic focusing is passing electron beam. In case of high-current mode, when electron beam space charge much more than space charge plasma lens the lens operates in plasma mode to create transparent plasma accelerating electrode and compensate space charge propagating electron beam. The lens magnetic field in this case uses for effective focusing beam.

In experiment was demonstrated a perspective applications of positive space charged PL with magnetic electron insulation for focusing and manipulating wide aperture high-current no relativistic electron beams (E_b = 16 keV; I_b = 100 A) [14]. Particularly, it was shown experimentally that under focusing these beams maximal compression factor was up to 30x, and beam current density at the focus was about 100 A/cm^2.

3. Plasma accelerator with open gas wall and closed electron drift

The accelerator with closed electron drift is one of the kinds of the electric rocket engines and devices for ion plasma treatment of the surface material. However, the accelerators with closed electron drift and open (gas) walls were not researched for now in contrast to the well-known and widely used plasma accelerators with anode layer and accelerators with closed electron drift and dielectric walls [15, 16]. Therefore, this type accelerator could be interested in manipulating high-current flow of charged particle as well as can be attractive for many different high-tech applications for potential devices of low-cost and compact thrusters. More than, it has some advantages since the wall absence leads to exclusion of the wall material inclusions into the ion beam and exclusion of the secondary electrons formation due to emission and thus to conservation of the plasma electrons dynamics.

The sample of plasma accelerator with closed electron drift and open walls is shown in **Figure 9** (left). This sample of cylindrical Hall-type plasma ion source that produced ion plasma flow converging toward the axis system was created for the properties exploration [17]. The discharge in the system burns due to ionization of the working gas by the electrons. Electrons are magnetized and formed stable negative space charge. The created ions accelerated from ionization zone to the cathode. As follow from discharge geometry an accumulation of ion space charge occurs as it is in the positive space charge lens (see above). The main part of generated ions leaves the system across radius, along with system axis, due to jets can appear

Figure 9. (a) Experimental sample: 1- cathode, 2- anode, and 3- permanent magnets system; (b)plasma jet in high-current operation mode.

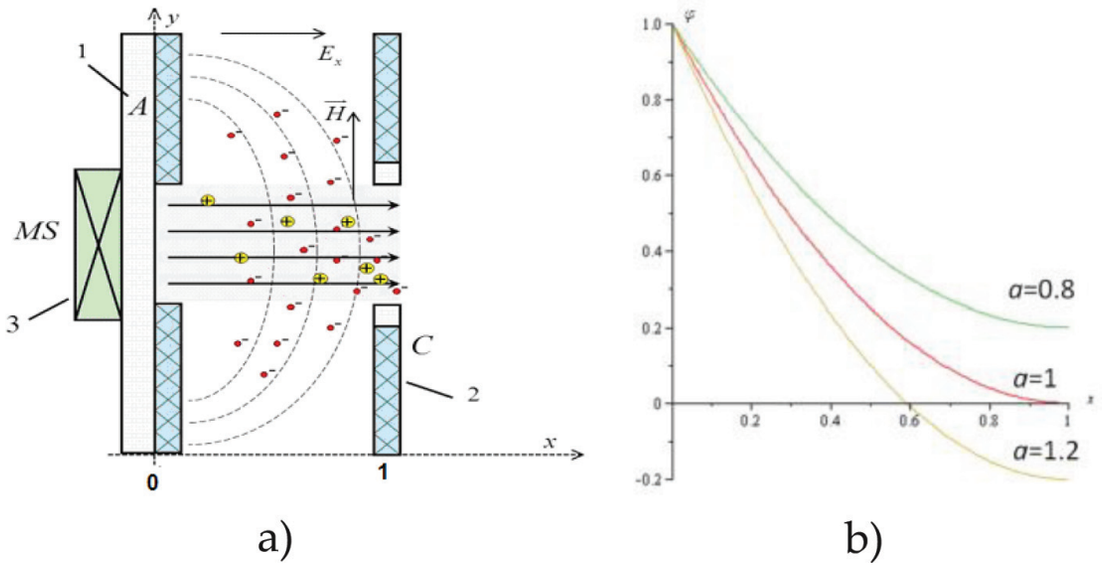

Figure 10. (a) Model of discharge gap: 1-anode, 2-cathode, 3-permanent magnets system; (b) potential distribution in the gap for different parameters *a* value.

on the edges of system. As follow from experiment [17, 18], the accelerator has two operating modes: low-current with narrow anode layer and clear-cut plasma flow and high-current when plasma fills the entire volume of the accelerator. The transfer to the high-current mode occurs under influence of two parameters: worked gas pressure and applied voltage. In high-current quasi-neutral plasma mode of accelerator operation, plasma jet is observed (see, **Figure 9** right). The preliminary results show that along the jet axis potential drop arise, which can be used for ion beam accelerating. The radial studies of plasma flow along system axis showed the significant increasing current density on the axis. It may indicate on plasma acceleration in that direction.

3.1. One-dimensional hydrodynamic and hybrid model

We will consider discharge gap, where ions production occurs due to ionization of the working gas by electrons (see **Figure 10a**). Electrons are magnetized, move along magnetic strength lines, and drift slowly to anode due to collisions. Ions are free and accelerated by electric field

move to the system axis. Will assume that the discharge current density in gap volume is the sum of the ion and electron components:

$$j_e + j_i = j_d \tag{8}$$

where j_i, j_e are ion and electron current density consequently:

$$j_i(x) = ev_i \int_0^x n_e(x)dx \tag{9}$$

$$j_e(x) = e\mu_\perp \left(n_e E(x) - \frac{d}{dx}(n_e T_e) \right) \tag{10}$$

ν_i-is the ionization frequency, $\mu_\perp = \frac{e\nu_e}{m\omega_{eH}^2}$ electron transverse mobility, $E(x) = -\frac{d\varphi}{dx}$-electric field, φ - potential, ν_e is the frequency of elastic collisions with neutrals and ions, ω_{eH} is the electron cyclotron frequency, T_e – electron temperature that could write in form [15]:

$$T_e(x) = \frac{\beta}{j_e(x)} \int_0^x j_e \frac{d\varphi}{ds} ds \tag{11}$$

for ion density we could write:

$$n_i(x) = \sqrt{\frac{M}{2e}} \int_0^x \frac{n_e(s)\nu_i ds}{\sqrt{\varphi(x) - \varphi(s)}} \tag{12}$$

and Poisson equation closed this system of equations:

$$n_e - n_i = \frac{1}{4\pi e}\varphi'' \tag{13}$$

In some cases equations system Eqs.(9) and (13) allows exact analytical solutions. Dimensionless these equations and assume that position x = 0 correspond to anode and initial potential on this boundary is equal applied voltage, position x = 1 correspond to cathode, and ion current on the cathode is equal to discharge current. If we neglect diffusion for case $n_e >> n_i$, that corresponds to a low-current mode, we can get exact solution in form [18, 19]:

$$\varphi = a\left((x-1)^2 - 1\right) + 1, a = \frac{\nu_i d^2}{2\mu_\perp \varphi_a} \tag{14}$$

where d is gap length. One can see that at the parameter $a = 1$, the total applied potential falls inside the gap (see **Figure 1b**). For this case, gap length is equal: $d = \sqrt{\frac{2\mu_\perp \varphi_A}{\nu_i}}$. Under assumption that electrons originated from the gap only by impact ionization, and go to the anode due to classical transverse mobility, last expression can rewritten in the form:

$$\delta = \rho_e(\varphi_A)\sqrt{\frac{2\nu_e}{\nu_i}} \tag{15}$$

This expression coincides with one for classical anode layer [20] accurate within √2. Note in case when parameter *a < 1 (*the gap length less than δ) potential drop is not completed (see **Figure 1b**). For case *a > 1,* when the gap length d > δ potential drop exceed applied potential. This can be due to the electron space charge dominated at the accelerator exit.

Another case is quasi-neutral plasma: $n_i \approx n_e$, that correspond to high-current mode [19]. In this case from the solution follows one interesting conclusion: when electron density does not change along the gap we could get generalization condition of self-sustained discharge in crossed electrical and magnetic fields (EXH), taking into consideration both electron and ion dynamics peculiarity. More than in this case solution for high-current mode is reduced to form (Eq. (14)) also. Even if we consider more general model description, assuming that electron heating losing occurs mostly by different kind of collisions it can show that potential distribution along gap weakly depend on electron temperature saving close to parabolic distribution. And under assumption that time of energetic losses equal electron lifetime in the gap we again come back to potential distribution (14) [18, 19].

For a more detailed study of the influence of ion dynamics on the system process, we applied a one-dimension mode hybrid model used for calculations of a span mode with neutral-particle ionization. In this model dynamics of ions and neutrals is described by kinetic equations, wherein right parts take into account only single ionizations:

$$\frac{\partial f_o}{\partial t} + v_0\frac{\partial f_0}{\partial x} = -\langle\sigma_{ie}v_e\rangle n_e f_0, \frac{\partial f_i}{\partial t} + v_i\frac{\partial f_i}{\partial x} + \frac{e}{M}E\frac{\partial f_i}{\partial v} = \langle\sigma_{ie}v_e\rangle n_e f_0 \tag{16}$$

where f_0, f_i distribution function of neutrals and ions consequently that satisfies boundary conditions:

$$f_0(0,v,t) = \frac{1}{(2\pi MT)^{3/2}}\exp\left(-\frac{Mv^2}{2T}\right), \mathrm{v} > 0; f_0(0,\mathrm{v},\mathrm{t}) = 0, \mathrm{v} < 0; f_i(0,\mathrm{v},\mathrm{t}) = 0 \tag{17}$$

Right part (Eq. (16)) we can write:

$$\langle\sigma_{ie}v_e\rangle = \sigma_{\max}v_e(T_e)\exp(-U_i/T_e), \tag{18}$$

where σ max – maximal ionization cross-section, ve(Te) – average electron thermal velocity, Ui – potential of ionization.

For electron part we will use hydrodynamic description and solve (Eqs. (8), (10), and(13)), where for ion density and current density is valid:

$$n_i = \int f_i dv, j_i = \int v_i f_i dv \tag{19}$$

The result of simulation hybrid model after achieving dynamic equilibrium by system in comparisons with hydrodynamic model is shown in **Figure 11**. One can see that taking into

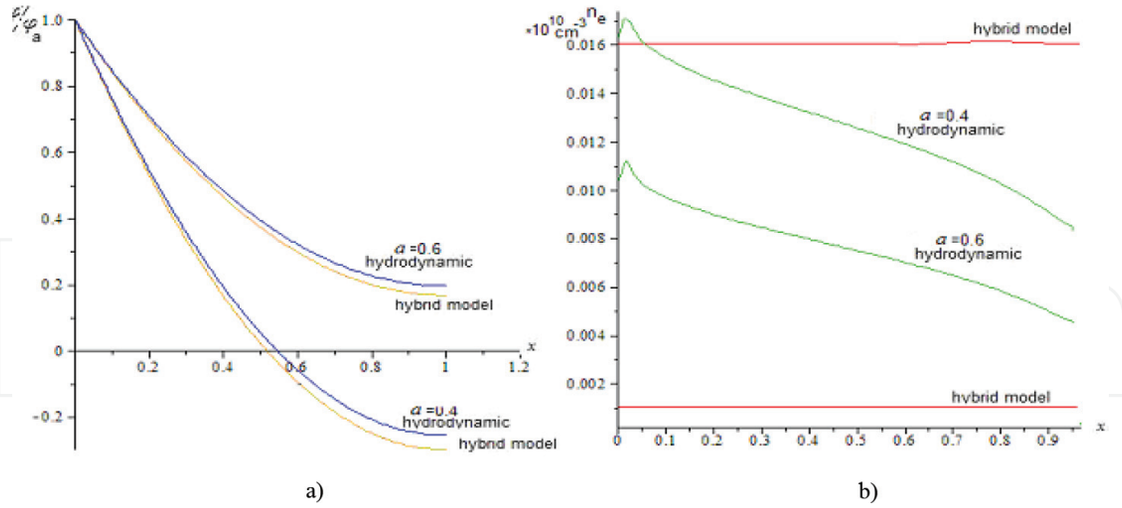

Figure 11. Comparison simulation results for hybrid and hydrodynamic models:(a) potential distribution in gap, (b) electron density.

account span mode with single ionization does not have a big impact on the result potential distribution (see **Figure 11a**). Electron density distribution (**Figure 11b**) looks more consistent along gap in hybrid model as compared to a hydrodynamic model. It is the result of influence on the system processes of neutrals dynamics and ionization, which are not taken into account in the hydrodynamic model.

Figure 12 shows ion density changing in the gap during the time in high-current mode (under applied anode potential equal 1200 V). It can be seen that at first ions number increases in near-anode region and remains almost constant in gap, then it increases almost linearly throughout the gap, and finally increases sharply at the cathode region.

Note that for correct description (especially high-current mode), it is necessary to model ionization and plasma creation, as well as motion of neutrals and formed ions in the whole volume of accelerator, thus need consider two-dimensional model.

3.2. Two-dimensional model

We will consider cylindrical geometry, where the anode is a cylinder with diameter 6.7 cm and applied potential about 1–2.5 kV, and cathode consist from two cylinders with diameter

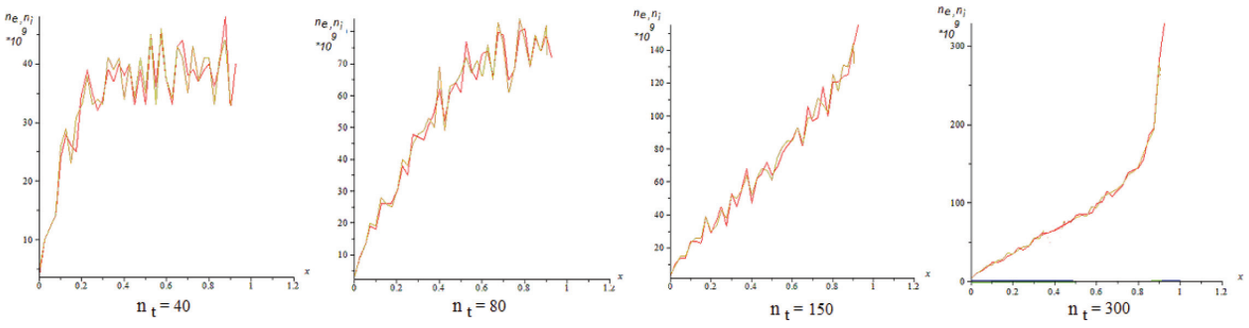

Figure 12. Ion density in the gap in high-current mode depending on time.

4.5 cm, spaced by some distance from each other. For ions and neutrals description we use Boltzmann kinetic equation:

$$\frac{\partial f_{i,n}}{\partial t} + \vec{\overline{v}}_{i,n}\frac{\partial f_{i,n}}{\partial \vec{r}} + \frac{e}{M}\left(E + \frac{1}{c}[v \times B]\right)\frac{\partial f_i}{\partial v_i} = St\left\{f_{i,n}\right\} \tag{20}$$

We solved this equation by splitting on the Vlasov equation for finding ions and neutrals trajectories:

$$\frac{\partial f_{i,n}}{\partial t} + \vec{\overline{v}}_{i,n}\frac{\partial f_{i,n}}{\partial \vec{r}} + \frac{e}{M}\left(E + \frac{1}{c}[v \times B]\right)\frac{\partial f_i}{\partial v_i} = 0 \tag{21}$$

and to correct the found trajectories taking into account the collision integral in which we took into account the processes of ionization and elastic and inelastic collisions:

$$\frac{Df_{i,n}}{Dt} = St\left\{f_{i,n}\right\} \tag{22}$$

The Vlasov equations were solved by the method of characteristics:

$$\frac{d\vec{v_k}}{dt} = \frac{q_k}{M}\left(\vec{E} + \frac{1}{c}[v_k \times B]\right], \frac{d\vec{r_k}}{dt} = \vec{v_k} \tag{23}$$

To solve these equations, the PIC method [10] with Boris scheme [11] was used to avoid singularities at the axis. For initial electric field distribution was taken electric field in the plasma absence: $E(r) = \frac{U_a}{r\ln(r_c/r_a)}$. The Monte-Carlo method was used for modeling of ionization in this field. The probability of a collision of a particle with energy ε_j during time Δt was found from expression [21]:

$$P_j = 1 - \exp\left(-v_j \Delta t \sigma(\varepsilon_j) n_j\left(\vec{r_j}\right)\right) \tag{24}$$

where $\sigma(\varepsilon)$ – collision cross-section (elastic, ionization or excitation), n_j – density of similar particles at the point r_j. To determine the probability of collision a random number β is chosen from interval [0,1] with the help of a random number generator. If $\beta < P_j$, then assumed that collision has occurred. It is determine the ratio of the cross-sections with the random number generator, which collision has occurred – elastic, excitation, or ionization. Independent of this particle parameters change or new ion adds in computational box. The emerging ions begin to move toward the system axis. The evolution of all particles that are in the modeling region is traced at each time step. For this motion, equations were solved, and new velocities and positions of the particles were found. Particles that move out the modeling box boundaries are excluded from consideration. After sufficiently long-time particle density distribution was found. The ion charge density and current density are calculated from coordinates and velocities of particles according to formulas:

$$\rho(r,t) = \frac{1}{V}\sum_j q_j R\left(\vec{r}, \vec{r_j}\ (t)\right), j(r,t) = \sum_j q_j v_j(t) R\left(\vec{r}, \vec{r_j}\ (t)\right) \tag{25}$$

where $R(r,r_j)$ – usual standard PIC – core, that characterizes particle size and shape and charges distribution in it. After that, the Poisson equation was solved, and new electric field distribution was found. Since electrons are magnetized we consider their movement in radial plane only, thus can solve for electrons one-dimensional hydrodynamic equations on each layer at z separately. Solve it we find electron density, calculate electric field on each layer and correct particle trajectories. After that, the procedure was repeated again. Modeling time is large enough for establish of ion multiplication process. The formation of the sufficient number of ions is possible due to magnetic field presence, which isolates anode from the cathode. Ions practically do not feel the magnetic field action and move from anode to the axis, where create a space charge, first in the center of the system. Electrons move along the magnetic field strength line, but due to collisions with neutrals, they start moving across the magnetic field. An internal electric field is formed, which slow down the ions and pushes out them from the volume along system axis. **Figure 13** shows results of modeling high-current mode (U_a = 1.2 kV, pressure 0.15 Pa, and magnetic field at the axis is 0.03 T). **Figure 13a** shows how the ions number to axis increases when ionization process is steady-state. One can see that number of ions increase not only to axis but also along axis from center to edge too. **Figure 13b** shows ion space charge distribution for different time step. One can see that ions create space charge in center of the system first, but then under electric field action they leave center and move along z-axis in both direction.

3.3. Conclusion remarks

First, the original approach to use plasma accelerators with closed electron drift and open walls for creation cost-effective low-maintenance plasma device for production converging toward axis accelerating ion beam was described. Based on the idea of continuity of current transferring in the system are found exact analytical solutions describing electric potential distribution along acceleration gap. It was shown that potential distribution is parabolic for different operation modes as in low-current mode as well as in high-current quasi-neutral plasma mode and cannot depend on electron temperature. It is found under conditions that everything electrons originated within the gap by impact ionization only, and go out at the anode due to mobility in transverse magnetic field, the condition full potential drop in the accelerating gap corresponds to equality gap length to the anode layer thickness. In case when the gap length less than anode layer thickness potential drop is not completed. For case when the gap length more than anode

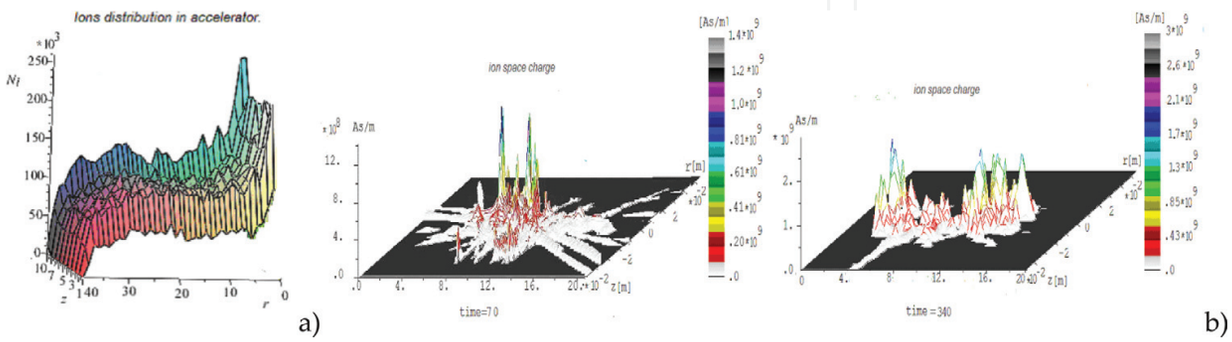

Figure 13. (a) Ions number dependence on r and z (r = 0,z = 0–center of the system); (b) ion space charge for time step 70 (left) and 340(right).

layer potential drop exceed applied potential. The generalization condition of self-sustained discharge in crossed ExH fields taking into consideration both electron and ion dynamic peculiarity were obtained. The performed modeling showed that in high-current mode the ions moving to the system center and then along the axis in both directions are able to create space charge. Experimental model of accelerator that formed ion flow converging toward the axis system was created [17, 18]. In high-current mode of accelerator operation is observed plasma jet. It is shown at the jet axis forms potential drop that could be used for ion beam accelerating. The experimental results are in good accordance with theory data.

Note also that the presented plasma device is attractive for many different high-tech practical applications, for example, like PL with positive space cloud for focusing negative, intense charge particles beams (electrons and negative ions), and for potential devices small rocket engines.

4. The model of the plasma-dynamical filter for micro-droplets eliminations

Now the vacuum-plasma technologies are widely used in erosion plasma sources, such as cathodic arc and laser-produced plasma, for thin films synthesis, and coatings with control properties. However, the micro-droplets present in the formed ion plasma flow restrict the applicability of this method of film synthesis. The micro-droplets component of erosion for the majority of metals is an essential part of general losses of the cathode material in a vacuum-arc, comparable with ion component. Therefore, for prevention of effect of micro-droplets on a substrate, it is necessary to eliminate droplets. The formation and propagation of micro-droplets, and also the mechanisms of decreasing of their effects on quality and rate deposition films and coatings were investigated in detail in works [22–26]. It is known from several approaches micro-droplets density reduction in ion plasma flows. Therefore, proposed methods do not provide the complete solution of the problem of micro-droplets elimination.

In paper Anders [26], the conclusion has been formulated that micro-droplets cannot be evaporated in the arc plasma flow without additional energy source. A new approach to the elimination or reduction of micro-droplets from the dense metal plasma flow based on the use of a cylindrical electrostatic PL configuration to generate an energetic radial electron beam within the low-energy ion plasma flow has been proposed and described in [27, 28]. The pumping of energy into arc plasma flow by the self-consistently formed radial beam of high-energy electrons for evaporation of micro-droplets could serve as additional energy source. The beam is formed by double layer, appeared in a cylindrical channel of the novel plasma-optical system in crossed radial electrical and longitudinal magnetic fields. Here we detailed describe the model of device for filtering dense plasma flow from micro-droplets.

4.1. Model approach

We will consider electrostatic PL configuration through which a low-energy arc ion plasma flow passes. **Figure 14** shows experimental device (left) and simplified model (right). A dense arc plasma flow with micro-droplets is propagated from the cathodic arc source and passes

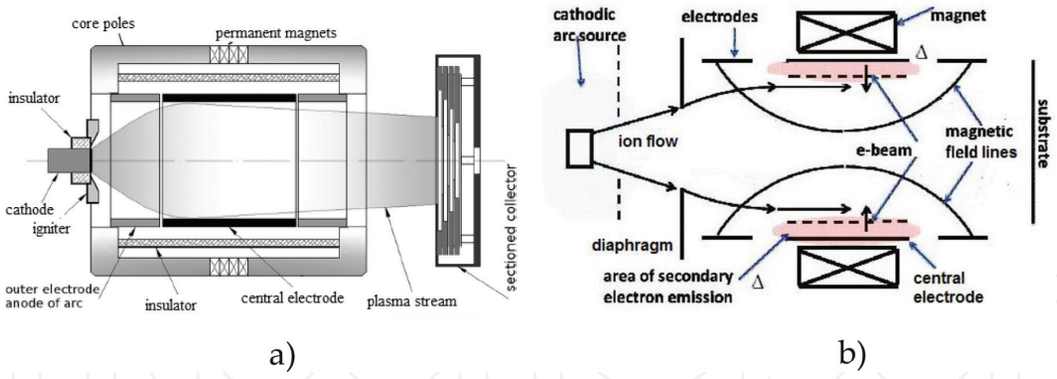

Figure 14. (a) Schema of the experimental set-up, (b) simplify model (Δ–spatial layer in which the strong radial electrical field is supported).

through diaphragm into the plasma-optical system. A part of the micro-droplets settles on the diaphragm, which is at the beginning of plasma-optical system, and remaining ones along with the flow propagate through the system.

The system consists of a cylinder (central electrode) of length L and diameter D on which the negative voltage U ∼ 1–3 kV is applied, and a pair of external ring grounded electrodes arranged symmetrically to the central electrode. The system is in the magnetic field of a short coil or permanent magnets. When arc plasma flow reaches the zone of the magnetic field action, it penetrates into the flow. The magnetic field must satisfy to the condition: $\rho_{Le} << D << \rho_{Li}$, where ρ_{Le}, ρ_{Li} – are the electron and ion Larmour radiuses. In such a magnetic field the electrons are magnetized, and ions are not magnetized. A dense plasma flow propagating inside the cylinder creates a thin wall layer Δ with a large radial electric field E_r. The magnetic field lines are equipotential inside flow, and electrical field, which created is similar to magnetic field lines. Because of the electrons of the flow are magnetized, they in the magnetic field are displaced to axis and prevent radial expansion of the flow. The density of flow increases with increasing of the magnetic field near axis, so control by magnetic field we can control by flow, keeping it from expansion.

High-energy electrons appear near the inner cylindrical surface by secondary ion-electron emission at this surface bombardment by peripheral flow ions. In result, the fast electrons beam created with current density $j_{eb} = \gamma j_{is}$ in near-wall layer (γ – secondary ion-electron emission coefficient).This electron beam injected from near-wall layer to plasma flow axis can serve as additional effective energy source for micro-droplet elimination.

4.2. Modeling and results

The modeling of high-energy radial electron beam formation was the first task of our consideration. For simulation, we used PIC-method with Boris scheme, analogically to previous section. The copper plasma flows transport through the plasma lens with applied potential −3 kV on the central electrode and magnetic field about 300–400 E was considered. **Figure 15a** shows initial plasma flow. The peripheral ions of flow collide with the inner wall of the central electrode and emitted electrons. The Monte-Carlo method was used for modeling emission

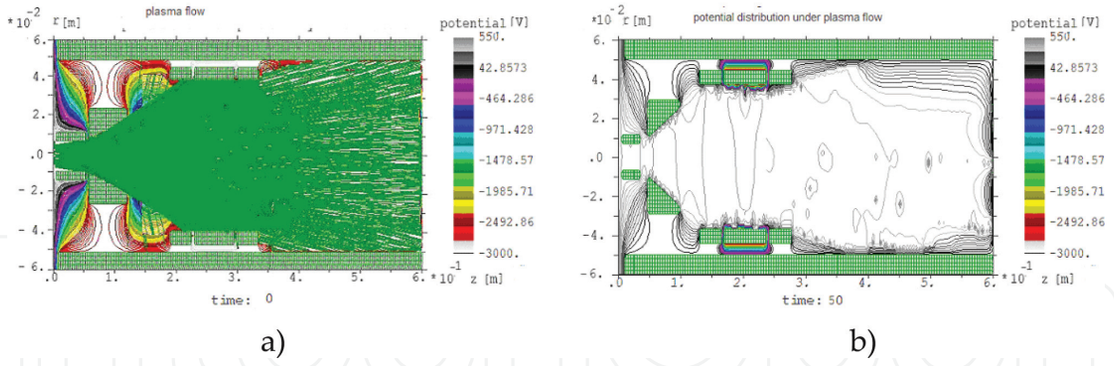

Figure 15. (a) Initial copper plasma flows, (b) potential distribution for time step 50.

process and electrons multiplication. The potential distribution is found by solving Poisson equation (see Eq.(7)). Ion density we find from the continuity equation: $div(j_i) = 0$. For electron density we can use expression: $n_e = n_{e0} \cdot \exp.(e\varphi/T_e)$, where n_{e0} – electron density of quasi-neutral plasma. For simplicity, we did not take into account the plasma heating and used finite T_e and T_i at the first stage. For all particles in the calculation box, the motion equations solve and find new positions and velocities. Part of the ions reaches the cathode and knocks out γ-electrons from it. We took them into account for Poisson equation solving too. We also take into account their ability to ionize when acquiring energy exceed the ionization energy. Very soon (in real time it corresponds to 1.6–2.5 μs) the potential jump near cathode is formed (see **Figure 15b**).

One can see that size of the potential jump layer is very small (about $5 \cdot 10^{-7}$ cm, so it is $<<\rho_{Le}$), thus electric field formed in the layer is large enough to accelerate the electrons to high-energy in the layer and force them to move toward the axis. We assumed the initial energy of emitted electron is 5 eV. Initial electrons move along magnetic field line as it shown in **Figure 16a**. However, due to appearance strong electric field in the layer, the average electron energy increases. It begins to exceed 10 eV at field strength is about 100 V/cm, and when electric field strength reaches about 500 V/cm it exceeds 100 eV. At such energies, the secondary electrons acquire the ability to ionize neutrals with the new secondary electrons appearance. As results, an avalanche-like ionization begins. Electrons move toward the axis and can accumulate there (see **Figure 16b**)). Note that application of the plasma lens to the transport of low-energy

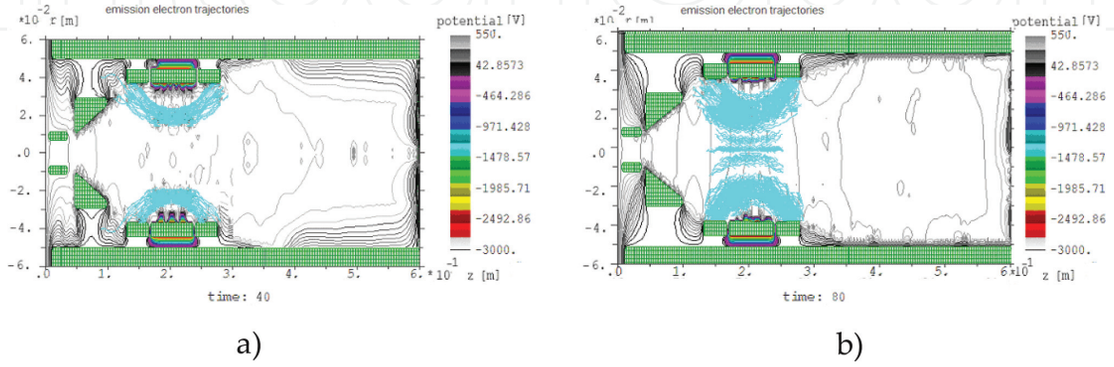

Figure 16. Trajectories of the emission electrons depends on time (a) $N_t = 40$, (b) $N_t = 80$.

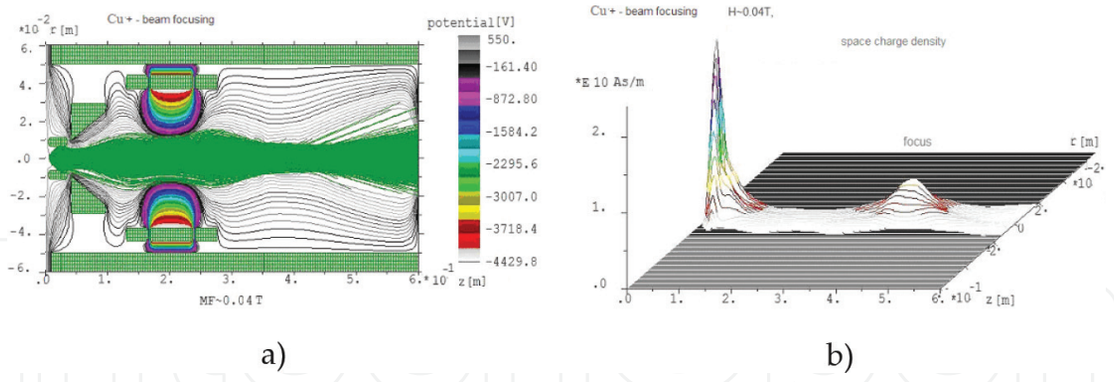

Figure 17. Influence radial electron beam on beam focusing: (a) trajectories of cu + beam; (b) space charge density in the beam.

high-current ion beam can improve the delivery of plasma flow to a substrate, as well as providing micro-droplet removal via the fast electrons within the lens region.

We considered the transport aspect and effect of fast electrons on transport characteristics low-energy ion plasma beam. **Figure 17** shows results of modeling transport copper ion beam with current 100A through plasma lens with presence of fast electrons in the volume. One can see that accumulation high-energy electrons on the axis and their space charge can provide additional compensation and focusing of the high-current ion beam.

4.3. Conclusion remarks

A new approach was proposed for the elimination of micro-droplets from the dense metal plasma, based on evaporation and thus removal of micro-droplets from the arc plasma by energetic electrons within the electrostatic PL. These electrons are generated self-consistently by secondary emission in the near-wall plasma layer from the internal surface of the lens central electrode and serves to evaporate, and thus remove micro-droplets from the plasma flow. The experiments [29] demonstrate the effectiveness of the electrostatic PL for focusing and manipulating wide-aperture, high-current, low-energy, streaming metal ion plasma flows. In these experiments, the self-sustained focusing of high-density, wide-aperture, low-energy ion plasma flow was observed. It has been shown that the presence of fast electrons in the volume of the plasma lens both improves the propagating ion plasma flow toward the substrate and introduces additional energy for effective evaporation and elimination of micro-droplets from the plasma flow.

5. Conclusions

We review some new results of development novel generation of cylindrical plasma devices based on the concept of magnetic insulation of electrons and equipotentialization magnetic field lines and an electrostatic PL configuration. The PL configuration of crossed electric and magnetic fields provides an attractive and suitable method for establishing stable plasma

discharge at low-pressure. Use of plasma lens configuration in this way was elaborated, explored and developed some cost efficiency, low-maintenance plasma devices for ion treatment, and deposition of exotic coatings with given functional properties. These devices make using permanent magnets and possess considerable flexibility with respect to spatial configuration. They can be operated as a stand-alone tool for ion treatment of substrates, or as part of integrated processing system together with cylindrical magnetron sputtering system, for coating deposition.

The research described has shown a principal possibility of a positive space charge cloud creation for negative charged particle beam focusing. It was demonstrated that possible create a positive space charge due to the magnetic electron insulation and reach strong focusing electric field, which sufficient for creation of short-focus elements to be used in systems for manipulating intense beams of negative ions and electrons. The further development of focusing properties of these devices demands study of intense negatively charged particle beams passing through the systems.

The simulations and experimental results demonstrate the high-efficiency of the electrostatic PL for focusing and manipulating wide aperture, high-current, low-energy, heavy metal ion plasma flow. These results open up new attractive way for further development and application erosion plasma sources for synthesis of exotic films and coatings with given functional properties. Some preliminary theoretical and experimental studies [27–29] have been carried out, providing confidence and optimism that the proposed idea for micro-droplet elimination has good potential for success.

Acknowledgements

This work was support by Grant NASU No PL-18 and No P-13_18.

Author details

Iryna Litovko[1]* and Alexey Goncharov[2]

*Address all correspondence to: ilitovko@ukr.net

1 Institute for Nuclear Research NAS of Ukraine, Kiev, Ukraine

2 Institute of Physics NAS of Ukraine, Kiev, Ukraine

References

[1] Morozov A. Focusing of cold quasi-neutral beams in electromagnetic fields. Doklady of the Academy of Sciences of the U.S.S.R. 1965;**163**(6):1363

[2] Morozov, Lebedev S. Plasmaoptics. In: Leontovich M, editor. Reviews of Plasma Physics. New York: Consultants Bureau; 1975

[3] Goncharov A, Dobrovolsky A, Zatuagan A, Protsenko I. High-current plasma lens. IEEE Transactions on Plasma Science. 1993;**21**(5):573

[4] Morozov AI, Semashko NN. On the mass separation of quasineutral beams. Technical Physics Letters. 2002;**28**(12):1052-1053

[5] Goncharov A, Brown I. High-current heavy ion beams in the electrostatic plasma lens. IEEE Transactions on Plasma Science. 2004;**32**(1):80

[6] Goncharov AA, Brown IG. Plasma devices based on the plasma lens-Areview of results and applications. IEEE Transactions on Plasma Science. 2007;**35**(4):986-991

[7] Goncharov A. The electrostatic plasma lens. Review of Scientific Instruments. 2013;**84**: 021101

[8] Goretskii V, Soloshenko I, Shchedrin A. Space charge lens for focusing negative-ion beams. Plasma Physics Reports. 2001;**27**(4):335-339

[9] Goncharov A, Evsyukov A, Dobrovol'skii A, Litovko I. Computer model for plasma devices based on the plasma lens configuration. Advances in Applied Plasma Science. 2007;**6**:5-8

[10] Potter D. Methods of Calculations in Physics. Moscow: Mir; 1975

[11] Boris JP, Lee R. Optimization of particle calculations in 2 and 3 dimensions, Communications in Mathematical Physics. 1969. 12. p. 131

[12] Goncharov A, Dobrovolskiy A, Dunets S, Evsyukov A, Litovko I, Gushenets V, Oks E. Positive-space-charge lens for focusing and manipulating high-current beams of negatively charged particles. IEEE Transactions on Plasma Science. 2011;**39**(6):1408-141113

[13] Goncharov AA, Dobrovolskiy AM, Dunets SP, Litovko IV, Gushenets VI, Oks EM. Electrostatic plasma lens for focusing negatively charged particle beams. The Review of Scientific Instruments. 2012;**83**(02B)

[14] Gushenets V, Goncharov A, Dobrovolskiy A, Dunets S, Litovko I, Oks E, Bugaev A. Electrostatic plasma lens focusing of an intense electron beam in an electron source with a vacuum arc plasma cathode. IEEE Transactions on Plasma Science. 2013;**41**(4, Part 3):2171-2174

[15] Morozov AI. Introduction to Plasmadynamics (Fismatlit, Moscow);2008. p. 572

[16] Goncharov AA, Brown IG. Physics and application of plasma accelerators. In: Morozov AI, editor. Minsk: Science and Technology; 1974

[17] Goncharov AA, Dobrovolsky AN, Naiko IV, Naiko LV, Litovko IV. Modes of plasma-dynamical system with closed electron drift and open walls. 2017 IEEE International Young Scientists Forum on Applied Physics and Engineering (YSF-2017). Book of papers YSF-2017, p. 267-270. DOI: 10.1109/YSF.2017.8126633

[18] Goncharov AA, Litovko IV, Dobrovolsky AN, Najko LV, Najko IV. Novel modification of hall-type ion source (study and the first results). Review of Scientific Instruments. 2016;**87**: 02A501

[19] Litovko IV, Goncharov AA, Dobrovolskiy AN, Naiko LV, Naiko IV. Modelling of new generation plasma optical devices. Nukleoika. 2016;**61**(2):207-212

[20] Grishin D, Leskov L, Kozlov N. Plasma Accelerators, Mashinostroenie, Moscow-231 c1983

[21] Vahedi V, Surendra M. A Monte Carlo collision model for the particle-in-cell method application for argon and oxigen discharges. Computer Physics Communications. 1995; **87**:179-198

[22] Anders A. Approaches to rid cathodic arc plasmas of macro- and nanoparticles: A review. Surface and Coatings Technology. 1999;**120**–**121**:319

[23] Boxman RL, Goldsmith S. Macroparticle contamination in cathodic arc coatings: Generation, transport and control. Surface and Coatings Technology. 1992;**52**:39

[24] Schülke T, Anders A. Velocity distribution of carbon macroparticles generated by pulsed vacuum arcs. Plasma Sources Science and Technology. 1999;**8**:567

[25] Aksenov II. The vacuum arc in erosion plasma sources. Kharkov: NSC KIPT. 2005:212

[26] Anders A. Growth and decay of macroparticles: A feasible approach to clean vacuum arc plasmas? Journal of Applied Physics. 1997;**82**:3679-3688

[27] Goncharov AA, Maslov VI, Fisk A. Novel plasma-optical device for the elimination of droplets in cathodic arc plasma coating. In: 55th Annual Technical Conference Proceedings of the Society of Vacuum Coaters (SVC); April 28-May 3, 2012; Santa Clara, California, USA. pp. 441–444

[28] Goncharov AA. Recent development of plasma optical systems (invited). Review of Scientific Instruments. 2016;**87**:02B901. DOI: 10.1063/1.4931718

[29] Bugaev A, Dobrovolskiy A, Goncharov A, Gushentets V, Litovko I, Naiko I, Oks E. Self-sustained focusing high-current heavy metal ion plasma flow produced by vacuum arc. Journal of Applied Physics. 2017;**121**(4):043301

IntechOpen